



# Enhanced heterogeneous wet hydrogen peroxide catalytic oxidation performance of fly ash-derived zeolite by CuO incorporation

E. Subramanian\* and N.L. Subbulekshmi

*Department of Chemistry, Manonmaniam Sundaranar University, Tirunelveli 627 012, Tamil Nadu, India.*

Received 29 September 2015; received in revised form 12 September 2016; accepted 4 March 2017

## KEYWORDS

Fly ash;  
 Zeolite NaX;  
 CuO;  
 Wet peroxide  
 oxidation;  
 Heterogeneous  
 catalysis;  
 Mineralization.

**Abstract.** Copper oxide incorporated fly ash-derived zeolite X (CuO/FAZ-X) was synthesized from solid waste coal fly ash by ion exchange with  $\text{Cu}^{2+}$  followed by calcination process. The synthesized materials were characterized by XRF, FTIR, SEM, EDX, and BET methods. In the application of the catalysts for wet peroxide oxidative decolorization of the model dye MB (Methylene Blue), the effects of major parameters, such as CuO loading, initial  $\text{H}_2\text{O}_2$  concentration, initial dye concentration, catalyst dosage, and pH, were investigated to assess the activity of the catalysts. In comparison with the activity of either fly ash-derived zeolite X (FAZ-X) or CuO, the combined catalyst (CuO/FAZ-X) showed an enhanced wet catalytic activity. Under the optimal condition (catalyst dose 250 mg/L, 100 ppm dye,  $\text{pH} = 6.8$ , 1 ml  $\text{H}_2\text{O}_2$ , and room temperature or  $30^\circ\text{C}$ ), the decolorization of MB was about 100% in 120 min by CuO/FAZ-X and only 31% and 44% by FAZ-X and CuO, respectively. Based on the decolorized products identified by HPLC-(ESI)-TOF-MS, the decolorization pathway of MB was proposed. Consequently, incorporation of CuO remarkably improved the catalytic activity of FAZ-X, such that CuO/FAZ-X emerged as a novel, reusable heterogeneous Fenton-like catalyst for oxidative decolorization of model dye MB. Thus, the present work demonstrates a simple and facile route for the conversion of waste coal fly ash into a valuable catalyst.

© 2017 Sharif University of Technology. All rights reserved.

## 1. Introduction

Industrial activities produce large amounts of dye- and pigment-containing effluent (wastewater), which is hazardous to the environment and has to be processed before being discharged into natural water bodies. These industrial effluents are intensely colored and associated with high level of chemical oxygen demand [1]. They not only deteriorate the aesthetics of receiving waters, but also pose significant threat to aquatic life due to the

hindrance in the penetration of oxygen and the formation of some toxic products by hydrolysis of dyes in the wastewater. The degradation/decolorization of dyes is, therefore, one of the challenging problems in the field of environmental science [2]. Several technologies are available to remove industrial organic wastes such as biological, thermal, and chemical processes, including adsorption, flocculation, membrane separation, oxidation, and so forth [3]. However, these technologies are non-destructive which result in secondary pollution and require further treatment [4].

Recently, Advanced Oxidation Processes (AOPs) have been considered as innovative technologies due to their *in-situ* generation of strong oxidant hydroxyl

\*. Corresponding author. Tel.: +91-99651 78458;  
 Fax: +91-462-2322973/2334363  
 E-mail address: esubram@yahoo.com (E. Subramanian)

radicals, which can mineralize almost all organic compounds to  $\text{CO}_2$ ,  $\text{H}_2\text{O}$ , and inorganic ions [4-6]. Various AOPs, such as Fenton or Fenton-like [4], Photo-Fenton [5], ultrasonication [6], ozonation [7], etc., have been developed and applied. Among all the developed AOPs, Catalytic Wet Peroxide Oxidation (CWPO) is recognized as a low-cost and environment-friendly technology, since it operates with simple equipment under ambient condition [8-10]. CWPO employs hydrogen peroxide ( $\text{H}_2\text{O}_2$ ) or other inorganic peroxides as an oxidation agent and a suitable catalyst to promote its partial decomposition to form radicals  $\text{HO}^\bullet$ ,  $\text{HO}_2^\bullet$ ,  $\text{O}_2^{\bullet-}$ , etc., which are all powerful oxidizing species able to efficiently degrade most of the organic pollutants present in wastewaters [9]. Moreover, hydrogen peroxide ( $\text{H}_2\text{O}_2$ ) is a non-toxic reactant which does not form any harmful byproduct, but improves the oxidation efficiency [11].

Homogeneous wet catalytic oxidation using Fenton's reagent ( $\text{Fe}^{2+}/\text{H}_2\text{O}_2$ ) and Fenton-like reagent ( $\text{Co}^{2+}/\text{H}_2\text{O}_2$ ,  $\text{Cu}^{2+}/\text{H}_2\text{O}_2$ , etc.) is normally employed to treat the organic pollutants in aqueous solutions. However, the ions-sludge generated in large quantity after the reaction and its removal at the end of treatment is inconvenient, and it is rather a costly process [10,11]. Further, in most cases, this homogeneous method is employed at high temperature and pressure which limits its practical application [12]. Therefore, heterogeneous catalysts functional at ambient condition with minimal leaching of active species under the reaction condition would be a better choice, and the same has now received wide attention [13,14].

Over the past few years, several heterogeneous Cu catalysts have been reported for  $\text{H}_2\text{O}_2$  activation. Most of them supported CuO systems using metal oxide, alumina, activated carbon, chitosan, zeolites, etc. For example, CWPO of a reactive dye by magnetic copper ferrite nanoparticles was evaluated by Tehrani-Bagha et al. [14]. Bradu et al. [15] studied the removal of azo dye by  $\text{CuO}/\text{Al}_2\text{O}_3$  and  $\text{NiO}/\text{Al}_2\text{O}_3$ . Alvarez et al. [16] reported wet air oxidation of phenol by  $\text{CuO}/\text{activated carbon}$  catalyst.  $\text{CuO}/\text{Zeolite}$  (synthesized from chemical precursors) was applied for the catalyzed oxidation of gaseous toluene [17], oxidation of secondary alcohols [18], adsorption [19], water oxidation of 2-chlorophenol [20], and photocatalytic activity [21]. In the last few years, various types of commercial, synthetic, and natural zeolites supporting metal oxides have been investigated, exhibiting high activity [17,21]. But, there is no report on the catalytic wet peroxide oxidation of organic dyes using  $\text{CuO}/\text{fly ash-derived zeolite NaX}$ .

Fly Ash (FA) is one of the solid wastes produced from the thermal power plant, which causes serious environmental problems [22]. In India, more than 120 million tons/year of FA is generated which tends to

increase every year, but only about 20-30% of it is used as an ingredient in Portland cement, clinkers, and fly ash bricks [23]. Hence, the management of fly ash becomes a matter of global concern from environmental and economic points of view. Fly ash consists of crystalline aluminosilicate, mullite, and  $\alpha$ -quartz with trace amounts of metal oxides depending on the nature of coal burn. Due to high silica and alumina content, FA can be converted into zeolite material by hydrothermal treatment [24], and this process is adopted in the present work with some modifications and also incorporation of CuO. Therefore, the aim and novelty of this work is the conversion of fly ash into phase-pure zeolite catalyst and the augmentation of its catalytic activity by nano CuO incorporation.

This paper focuses mainly on three aspects:

- (i) Synthesis and characterization of fly ash-derived zeolite X (FAZ-X) and  $\text{CuO}/\text{FAZ-X}$  heterogeneous catalysts;
- (ii) Evaluation of their adsorption and catalytic oxidative decolorization of a model dye Methylene Blue (MB);
- (iii) Investigation of optimal conditions of several experimental factors such as CuO loading, initial dye concentration, catalyst dosage, initial peroxide concentration, and pH.

The merits of this work are:

- (i) Utility of low or zero cost material coal fly ash for zeolite synthesis and helping the environmental remediation;
- (ii) CWPO at room temperature and atmospheric pressure condition;
- (iii) A simple and facile route to prepare FAZ-X and further incorporation of nano CuO into FAZ-X.

The results indicate that the designed and developed  $\text{CuO}/\text{FAZ-X}$  catalyst proves its worthiness in many respects such as efficiency, stability, reliability, and above all environmental remediation of the waste material coal fly ash.

## 2. Experimental

### 2.1. Materials

The main raw material, i.e. coal Fly Ash sample (FA), was collected from electrostatic precipitators of nearby thermal power plant at Tuticorin, Tamil Nadu. The commercially available chemicals used in the present work were sulphuric acid (LOBA chemie, India), methylene blue (Rankem, India), sodium hydroxide (LOBA chemie, Mumbai), cupric sulphate (Merck, Mumbai), hydrochloric acid (Merck, Mumbai), potassium dichromate (Merck, Mumbai), ferrous sulphate

(Merck, Mumbai), silver sulphate (Qualigens Fine Chemicals, Mumbai), and Ferroin indicator (Rankem, India). All the procured chemicals were used without further purification as they were of analytical grade. Stock solution 1000 mg/L (1000 ppm) of methylene blue was prepared in Doubly Distilled water (DD water) and diluted to desired concentration during decolorization experiments. Throughout the experiment, DD water was used. pH of the dye solution was adjusted with aqueous HCl and NaOH solutions.

## 2.2. Pretreatment of FA

The raw fly ash samples were first screened through BSS Tyler sieve of 75 mesh size to eliminate larger particles. First, the FA was washed with DD water several times. Then, the water washed FA was treated with 0.1 M aqueous HCl to facilitate zeolite formation and to decrease the concentration of metal oxides (alkali oxides) which were mainly present on the exterior part of fly ash particles. This acid treatment also served to increase the activity, thermal stability, and acidity of the zeolite, all aiming for better catalytic activity. The treated FA, thus, is called Pre-treated Fly Ash (PFA).

## 2.3. Synthesis of Zeolite NaX (FAZ-X)

Zeolite NaX was synthesized from FA (pretreated) by fusion method, which involved alkali fusion followed by hydrothermal treatment [23,24]. A typical procedure is given below: the pretreated FA was mixed with sodium hydroxide at 1:1.3 ratio (wt/wt) and fused at 550°C for 1 h. Thereafter, the fused product was mixed with DD water, and the resulting slurry was aged for 20 h, and finally crystallized at 90°C for 6 h. The solid product was recovered by filtration and washed with DD water until the pH of the washings was about 9. The product was then dried in a hot air oven at 110°C for 2-3 h. The sample is labeled as FAZ-X.

## 2.4. Synthesis of CuO/FAZ-X

For preparing CuO/FAZ-X, 3 g of FAZ-X was suspended in 100 ml of 0.1 M cupric sulphate solution. The reaction mixture was magnetically stirred for 20 h. The obtained Cu(II) exchanged zeolite (Cu/FAZ-X) was separated by filtration (whatman No. 1 paper) and washed several times with DD water to remove all water-soluble remaining ions in the product. Resultant product was transferred to a silica crucible and placed in an oven at 100±5°C for 12 h. Finally, it was calcined in a pre-heated muffle furnace at 450°C for 4 h. The sample was then cooled to room temperature, ground to fine powder, and stored in air-tight vials. This is labeled as CuO/FAZ-X.

## 2.5. Synthesis of different levels CuO loaded FAZ-X

The procedure described in Section 2.4 was followed with different concentrations of cupric sulphate so-

lution (0.05, 0.5, and 1.0 M), and the remaining procedure is the same as the previous ones. The synthesized materials are labeled as 0.05 M, 0.5 M, and 1.0 M CuO loaded FAZ-X.

## 2.6. Synthesis of CuO

Copper (II) solution (0.1 M) with cupric sulphate was prepared in double distilled water, stirred and heated to 100°C. Then, 1.0 M NaOH was added drop-wise to this solution till pH 7. A brownish-black precipitate was obtained, filtered, washed thoroughly with DD water and dried at 100°C overnight. Finally, the sample was heat-treated in a muffle furnace at 450°C for 4 h. Then, it was allowed to cool down to room temperature, ground to fine powder, and stored in air-tight vials.

## 2.7. Materials characterization

Powder X-Ray Diffraction (XRD) patterns were recorded for angle  $2\theta = 10 - 80^\circ$  in a step of  $0.05^\circ$  in a continuous scanning mode using the instrument, PANalytical Expert Pro-MPD with  $\text{CuK}_\alpha$  radiation ( $\lambda = 1.5406 \text{ \AA}$ ) from a generator set at 30 mA and 40 KV. The chemical composition of FA, PFA, FAZ-X, and CuO/FAZ-X was analyzed by wavelength dispersive X-Ray Fluorescence spectroscopy (XRF) instrument S8 TIGER from Bruker, Germany. FTIR spectra of the samples were recorded (in spectral grade KBr pellet) with FTIR spectrometer (JASCO FTIR-410) in the wavenumber range  $400\text{--}4000 \text{ cm}^{-1}$  at a resolution of  $2 \text{ cm}^{-1}$ . The specific surface area of the powder samples was determined by BET and Langmuir nitrogen adsorption/desorption method in Micromeritics ASAP 2420 surface area analyzer. SEM (Scanning Electron Microscope) images of the samples were obtained by VEGA 3 TESCAN microscope. The integrated Energy Dispersive X-ray (EDX) spectroscopy was applied to identify the dispersion of copper in CuO/FAZ-X sample using BRUKER instrument. UV-visible spectra of the decolorized solution of methylene blue were obtained in the wavelength range 200–800 nm on Perkin-Elmer spectrophotometer, Lambda 25 model. The oxidized products of MB were analyzed by Alliance 2795 HPLC coupled with a Waters Micromass Quattro triple quadrupole mass spectrometer equipped with electrospray ionization (ESI) and Atmospheric Pressure Chemical Ionization (APCI) sources having mass range up to 4000 amu in quadrupole and 20000 amu in TOF.

## 2.8. Catalytic evaluation

The catalytic oxidation of MB dye was carried out under ambient condition. The reaction was conducted in a three-necked flat bottom flask with constant stirring at around 300 rpm. The flask was covered and wrapped with aluminum foil to block the incidence of indoor light on the reaction mixture. In a typical experiment, 50 mg catalyst powder was dispersed in

200 ml MB solution ( $100 \text{ mgL}^{-1}$ ). At the natural pH 6.8 (prior to the addition of  $\text{H}_2\text{O}_2$ ), the suspension was magnetically stirred for about 30 min to establish the adsorption/desorption equilibrium between dye and catalyst. Then, the required amount of 30% v/v  $\text{H}_2\text{O}_2$  was added to the above suspension under continuous magnetic stirring. At the given time intervals (10 min), 1 ml aliquot was collected and immediately centrifuged to remove the catalyst and for subsequent spectral analysis of the dye solution. The decolorization was monitored by UV-Visible spectroscopy at 665 nm, the maximum absorption wavelength of MB using Eq. (1):

$$\text{Decolorization \%} = \frac{(A_o - A_t)}{A_o} \times 100, \quad (1)$$

where  $A_o$  is the initial absorbance of dye, and  $A_t$  is the absorbance at selected time intervals.

The catalytic decolorization of MB was investigated for the influence of experimental variables such as CuO loading on FAZ-X, initial  $\text{H}_2\text{O}_2$  concentration, initial concentration of MB, catalyst dose, and pH. To run the catalyst recycle, the used catalyst was collected by centrifugation, washed with water, dried at  $100^\circ\text{C}$ , and then used for MB decolorization. This was repeated for several cycles of the decolorization experiment.

COD load of the reaction mixture was monitored during the oxidation reaction by the open dichromate reflux method [25(a)]. In this method, 10 ml of the reaction mixture was mixed with 25 ml of 0.01467 M  $\text{K}_2\text{Cr}_2\text{O}_7$  reagent, 35 ml conc.  $\text{H}_2\text{SO}_4$  and a pinch of silver sulphate. The mixture was refluxed for 2 h, cooled, and titrated with 0.05 M ammonium ferrous sulphate (FAS) solution using ferroin indicator. The whole procedure was repeated with a blank taking 10 ml of distilled water in place of the reaction mixture. COD was computed by the following equation:

$$\text{COD as mg O}_2/\text{L} = \frac{(A - B) \times M \times 8000}{V}, \quad (2)$$

where:

|      |  |
|------|--|
| $A$  | Volume of FAS used for blank titration,                        |
| $B$  | Volume of FAS used for sample titration,                       |
| $M$  | Molarity of FAS,   |
| $V$  | Volume of the reaction mixture,                                |
| 8000 | Milli equivalent weight of oxygen $\times 1000 \text{ ml/L}$ . |

The COD removal was calculated by Eq. (3):

$$\% \text{COD} = \frac{(\text{COD}_o - \text{COD}_t)}{\text{COD}_o} \times 100, \quad (3)$$

where  $\text{COD}_o$  = COD of the reaction mixture at  $t = 0$  (i.e., before commencement of oxidation) and  $\text{COD}_t$  = COD of the reaction mixture at  $t = t$  (i.e., after oxidation proceeded for time,  $t$ ).

### 3. Results and discussion

#### 3.1. Materials characterization

##### 3.1.1. XRF analysis

Table 1 presents the chemical composition of various materials derived from XRF analysis. According to the American Society for Testing Materials (ASTM) [25(b)], the FA material used in this study is classified as sialic type because it contains less than 5% CaO and > 90% of the three main components ( $\text{SiO}_2$ ,  $\text{Al}_2\text{O}_3$ , and  $\text{Fe}_2\text{O}_3$ ) combined. A perusal of data in Table 1 reveals the following:

- Pretreatment of FA with acid has reduced the amount of iron, calcium, and magnesium oxides by leaching;
- Alkali fusion and hydrothermal treatment of FA has considerably increased the content of  $\text{Na}_2\text{O}$  (from mere 0.16 to 18.3%);
- However, Cu(II) ion exchange and subsequent calcination has substantially removed  $\text{Na}_2\text{O}$  by substituting it with CuO.

Other metal oxides have also undergone a considerable decrease in their content. Thus, the synthesis process and the expected chemical change in each and every step of CuO/FAZ-X formation are confirmed and validated by XRF analysis.

##### 3.1.2. XRD studies

The X-Ray Diffraction (XRD) patterns of PFA and FAZ-X are shown in Figure 1. The characteristic high

**Table 1.** Chemical composition (in wt%) of Fly Ash (FA), Pre-treated FA (PFA), Fly Ash-derived Zeolite (FAZ-X) and CuO incorporated FAZ-X (CuO/FAZ-X) resulted from XRF analysis.

| Chemical compound       | FA    | PFA   | FAZ-X | CuO/FAZ-X |
|-------------------------|-------|-------|-------|-----------|
| $\text{SiO}_2$          | 58.58 | 60.13 | 43.41 | 38.18     |
| $\text{Al}_2\text{O}_3$ | 30.19 | 29.64 | 28.81 | 27.09     |
| $\text{Na}_2\text{O}$   | 0.16  | 0.13  | 18.30 | 0.56      |
| $\text{Fe}_2\text{O}_3$ | 5.63  | 5.26  | 5.43  | 1.78      |
| $\text{TiO}_2$          | 1.64  | 1.65  | 1.74  | 1.58      |
| CaO                     | 1.25  | 0.81  | 0.93  | 0.27      |
| MgO                     | 1.01  | 0.89  | 0.75  | 0.74      |
| $\text{K}_2\text{O}$    | 1.42  | 1.39  | 0.55  | 0.13      |
| BaO                     | 0.08  | 0.07  | 0.06  | 0.07      |
| CuO                     | 0.02  | 0.01  | 0.01  | 29.57     |

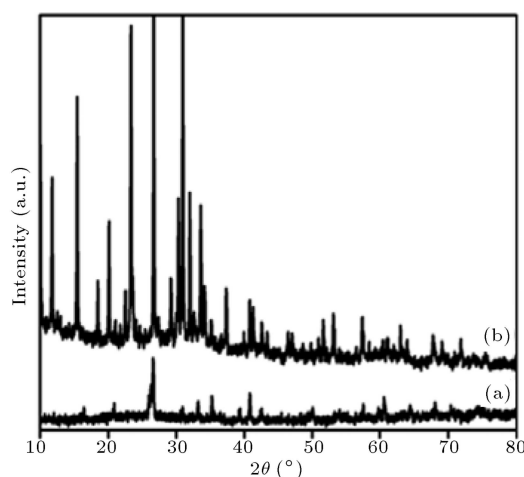


**Figure 1.** XRD patterns of (a) PFA and (b) FAZ-X.

intense peaks at  $2\theta = 26.6^\circ$  and  $40.9^\circ$  together with other major peaks (Figure 1(a)) are indicative of the presence of Quartz (Q) and Mullite (M) in PFA. The diffraction pattern of PFA is in good agreement with JCPDS file No. 001-0649. The characteristic lines located at  $2\theta$  values of 10.1, 11.8, 15.5, 18.4, 20.09, 23.3, 26.65, 29.21, 30.3, 31.1, 32.6, 37.4,  $41.2^\circ$ , etc., in XRD pattern (b) in Figure 1 can be indexed to NaX zeolite crystalline planes by matching it with the zeolite pattern in the library of XRD patterns [JCPDS No. 39-0218] and also by matching it with reports in the literature [23,24]. The most distinct changes in the XRD pattern of FAZ-X, when compared to PFA, are the disappearance of the quartz and mullite peaks and the appearance of new crystalline phase corresponding only to zeolite X.

### 3.1.3. FTIR studies

Figure 2 shows the FTIR spectra of PFA, FAZ-X, and CuO/FAZ-X; Table 2 compiles the IR bands. The mid-

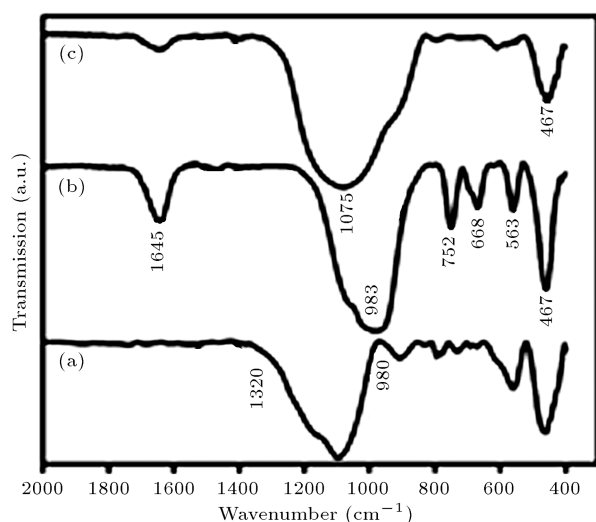


**Figure 2.** FTIR spectra of (a) PFA, (b) FAZ-X, and (c) CuO/FAZ-X.

**Table 2.** IR peak assignments of FAZ-X and CuO/FAZ-X materials.

| IR assignments          | Wavenumber ( $\text{cm}^{-1}$ ) |
|-------------------------|---------------------------------|
| <b>FAZ-X material:</b>  |                                 |
| Internal tetrahedral:   |                                 |
| Asymmetric stretch      | 1250-950                        |
| Symmetric stretch       | 720-650                         |
| T-O band [T = Si or Al] | 420-500                         |
| External linkage:       |                                 |
| Double ring             | 650-500                         |
| Pore opening            | 300-420                         |
| Symmetric stretch       | 750-820                         |
| Asymmetric stretch      | 1050-1150 (sharp)               |
| <b>CuO/FAZ-X:</b>       |                                 |
| CuO band                | 369, 906, 610, 517 and 429      |
| Deformation of water    | 1625-1640                       |

infrared region of the spectra ( $1500\text{--}500\text{ cm}^{-1}$ ) contains the fundamental framework vibration of  $\text{Si}(\text{AlO}_4)$  groupings. The in-between broadband within the wavenumbers of 980 and  $1320\text{ cm}^{-1}$  in the IR spectrum of PFA (Figure 2(a)) represents the presence of substituted Al atoms in the tetrahedral forms of silica frameworks [23]. Figure 2(b) shows the broad peak with high intensity at  $983\text{ cm}^{-1}$  and sharp peak at  $752\text{ cm}^{-1}$  attributed to Si-Al-O asymmetric and symmetric stretching vibrations, respectively. The band at  $1645\text{ cm}^{-1}$  is assigned to the asymmetric and symmetric bending/deformation vibrations of O-H, suggesting the presence of possibly hydrated aluminum silicates. All these observations confirm the formation of X-type zeolite on alkali treatment of FA [23,24]. A specific band at  $2369\text{ cm}^{-1}$  (not shown in Figure 2(c)) appearing for calcined sample (CuO/FAZ-X) suggests the existence of CuO in the zeolite structure [26]. The band at about  $983\text{ cm}^{-1}$  in the spectra of FAZ-X (Figure 2(b)) is shifted to high wavenumber  $1075\text{ cm}^{-1}$  (Figure 2(c)) indicative of exchanging  $\text{Na}^+$  by  $\text{Cu}^{2+}$  cations [27,28]. All the above-mentioned peaks, except the broadband at  $1075\text{ cm}^{-1}$ , appear either weak or overlapped/merged with neighboring peaks or shifted to higher wavenumber side in CuO/FAZ-X (Figure 2(c)) [29,30]. Thus, IR spectra provide evidence for zeolite formation from PFA, and then CuO/FAZ-X from FAZ-X.

### 3.1.4. SEM and EDX analysis

The SEM images of FA, FAZ-X, and CuO/FAZ-X samples are shown in Figure 3. Fly ash consists of smooth surfaced spherical particles in size range of  $0.5\text{--}3.0\text{ }\mu\text{m}$  (Figure 3(a)). SEM image of FAZ-X pow-

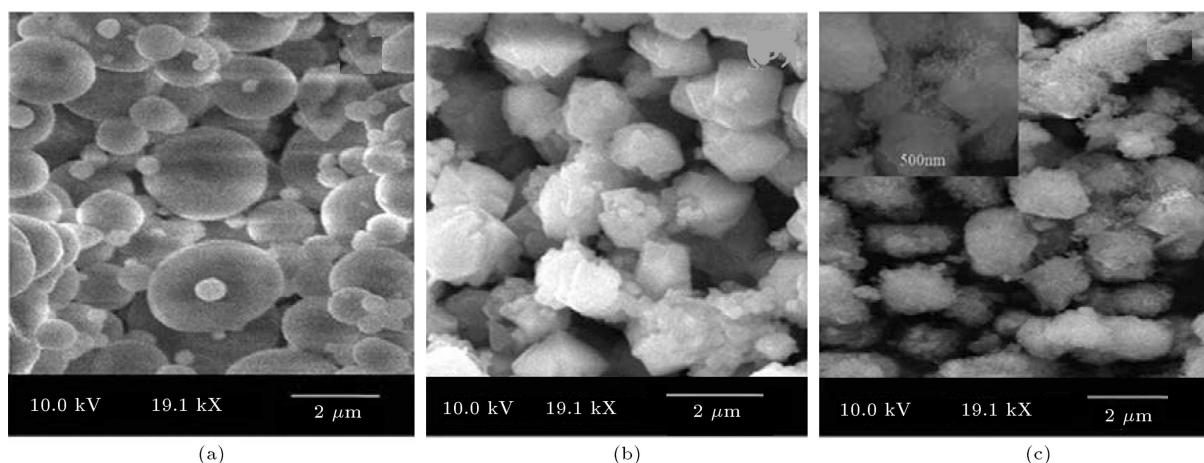


**Figure 3.** SEM images of (a) FA, (b) FAZ-X, and (c) CuO/FAZ-X (inset-magnified image showing CuO nano fringes).

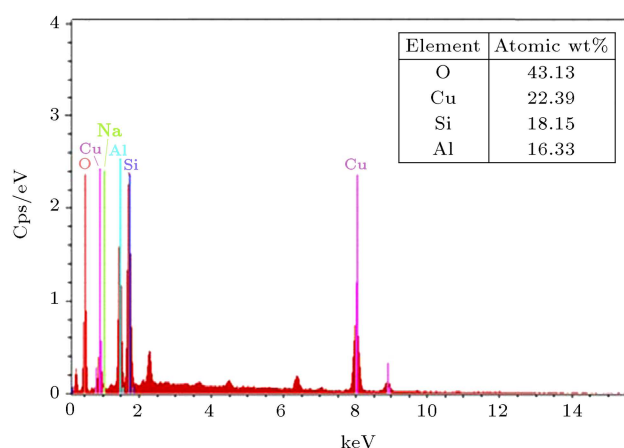


**Figure 4.** EDX spectra and EDX analysis report of CuO/FAZ-X.

der (Figure 3(b)) consists of predominantly spherical, smooth particles/grains of 1–2  $\mu\text{m}$  in diameter [24]. However, the image of CuO/FAZ-X (Figure 3(c)) shows irregularly shaped somewhat bigger spongy such as particles. A close examination of the enlarged image (inset in Figure 3(c)) reveals the existence of nano fringes (small densely arranged fiber-like structure) on the entire surface of FAZ-X particles. The whole morphology of CuO/FAZ-X appears as the white spongy fully opened cotton fruit in the plankton.

The EDX spectra of CuO/FAZ-X are shown in Figure 4. The spectra show sharp signals corresponding to all the expected elements. The elemental analysis data of Figure 4 clearly suggest the chemical composition of the materials. The low Si/Al ratio of zeolite (1.5) confirms the formation of Zeolite NaX type. The presence of 22 atomic % of Cu which is close to the XRF result of 26.88 wt% for CuO confirms the formation of CuO/FAZ-X with a higher CuO dispersion. Thus, EDX analysis provides evidence for the elemental composition of synthesized zeolite materials.

**Table 3.** Surface area, pore volume, and pore radius of FAZ-X and CuO/FAZ-X.

|  | FAZ-X | CuO/FAZ-X |
|--|-------|-----------|
| Surface area ( $\text{m}^2/\text{g}$ )       | 413   | 58        |
| Total pore volume ( $\text{cm}^3/\text{g}$ ) | 0.22  | 0.19      |
| Average pore radius ( $\text{\AA}$ )         | 29    | 50        |

### 3.1.5. BET studies

The surface area, pore volume, and pore size of FAZ-X and CuO/FAZ-X catalyst samples obtained from BET  $\text{N}_2$  adsorption/desorption method are entered into Table 3. BET surface area of CuO/FAZ-X and FAZ-X are found to be 58  $\text{m}^2/\text{g}$  and 413  $\text{m}^2/\text{g}$ , respectively. The surface area of FAZ-X decreases significantly, while pore volume decreases only slightly on CuO loading. These results are clearly logical because the introduced CuO species occupy and cover the zeolite pores, channels, and cavities as observed from the SEM images (Figure 3). They also adhere to the surface of zeolite particles. Hence, the zeolite particles are bulged and the increase in size explains the considerable increase in pore size or radius (Table 3).

### 3.2. Assessment of adsorption and decolorization efficiency of CuO/FAZ-X, CuO, and FAZ-X

Figure 5(a) shows the adsorption of MB dye under dark condition over FAZ-X, CuO, and CuO/FAZ-X catalysts. The amounts of adsorption of the catalysts are 3% for CuO/FAZ-X, 40% for FAZ-X, and 0.1% for CuO after 180 min contact time. The results reveal that FAZ-X has greater adsorption for MB dye compared to CuO or CuO/FAZ-X. Pristine CuO is a very poor adsorbent (almost no adsorption) for MB. This feature considerably reduces the adsorption tendency of FAZ-X on CuO incorporation, and consequently, CuO/FAZ-X, as the newly developed catalyst, has only a physically poor adsorption for MB.



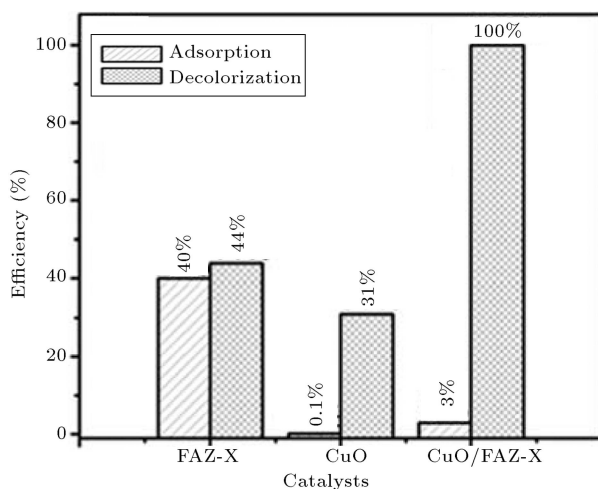


**Figure 5a.** Effects of various catalysts (FAZ-X, CuO, and CuO/FAZ-X) on MB decolorization (conditions: 5 ml/L  $H_2O_2$ , 250 mg/L catalyst, 100 ppm dye, and pH 6.8).

Figure 5(a) also illustrates the performance of wet catalytic activities of CuO/FAZ-X, FAZ-X, and CuO for the oxidation and decolorization of MB with  $H_2O_2$  under ambient condition.  $H_2O_2$  alone shows no significant activity for MB decolorization (7%) in 120 min. In contrast, remarkable improvement of MB decolorization occurs with CuO/FAZ-X/ $H_2O_2$  suspension, and about 100% of MB is decolorized in 120 min at natural pH (6.8). But, FAZ-X and CuO exhibit respectively, 31% and 44% MB decolorization after 120 min reaction time. Therefore, it is obvious that the combination of CuO and zeolite NaX (FAZ-X) results in synergic effect on catalytic activity leading to almost doubling the activity and complete decolorization of MB.

### 3.3. Decolorization of MB under different experimental variables

#### 3.3.1. Effect of CuO loading

Influence of CuO loading on the catalytic oxidation of MB is shown in Figure 5(b). Dye decolorization increases with the increase in CuO loading up to 0.1 M  $Cu^{2+}$  concentration, and thereafter, the decolorization % decreases possibly due to more aggregation of CuO species on the surface of FAZ-X. As evident from the data in Table 3, more aggregation reduces the surface area of the catalyst resulting in a decrease in a number of active sites present on the catalyst. Hence, there is a less amount of production of hydroxyl radicals accounting well for the low catalytic activity [31]. All further studies were done with CuO/FAZ-X catalyst where CuO was loaded using 0.1 M Cu(II) solution which is found to be optimal.

#### 3.3.2. Effect of catalyst dosage

The effect of catalyst dosage on the decolorization of MB is shown in Figure 5(c). Increase in decolorization with increase in catalyst dosage is observed. This could

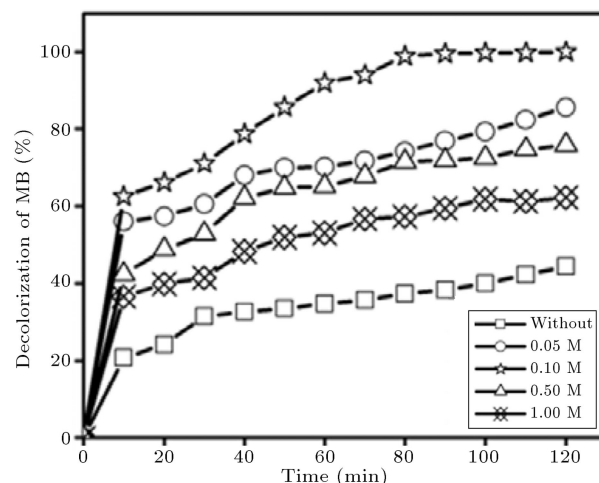


**Figure 5b.** Effects of different levels of CuO loading on MB decolorization by CuO/FAZ-X (conditions: 5 ml/L  $H_2O_2$ , 250 mg/L catalyst, 100 ppm dye, and pH 6.8).

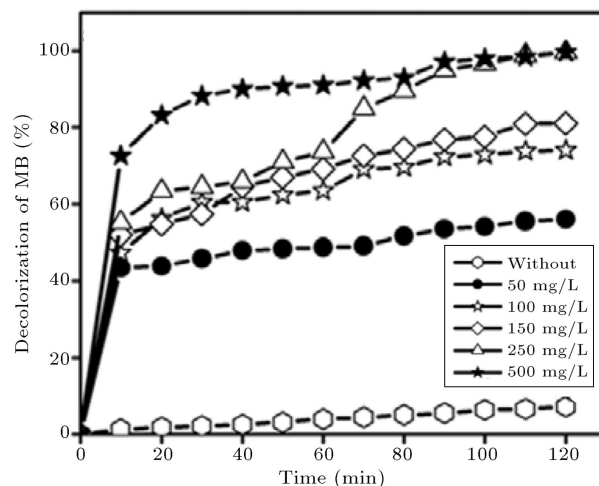
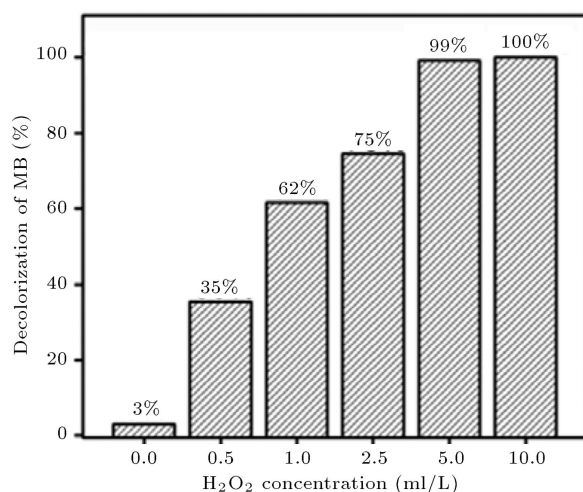


**Figure 5c.** Effect of catalyst dosage on MB decolorization by CuO/FAZ-X (conditions: 5 ml/L  $H_2O_2$ , 100 ppm dye, and pH 6.8).

be understood by the presence of more active sites for generation of free-radical species, which in turn can promote the decolorization extent and yield [32,33]. Maximum dye decolorization (100%) is observed at a catalyst dosage of 250 mg/L.

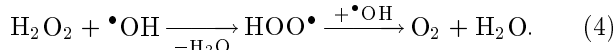
#### 3.3.3. Effect of $H_2O_2$ concentration

Figure 5(d) illustrates the influence of  $H_2O_2$  concentration on the decolorization of MB dye using CuO/FAZ-X. It is clear that the decolorization efficiency increases with increase in  $H_2O_2$  concentration from 0.5 to 10 ml/L. The maximum decolorization efficiency (100%) is obtained at 10 ml/L  $H_2O_2$  in 60 min. When using minimum amount (5 ml/L) of  $H_2O_2$ , 100% decolorization occurs in 120 min. At very low concentration,  $H_2O_2$  could not generate the sufficient number of  $\bullet OH$  radicals, which slows down the oxidation rate, and hence reduces the decolorization efficiency. Higher con-



**Figure 5d.** Effect of initial H<sub>2</sub>O<sub>2</sub> concentration on MB decolorization by CuO/FAZ-X (conditions: 250 mg/L catalyst, 100 ppm dye, and pH 6.8).

centration of H<sub>2</sub>O<sub>2</sub> (10 ml/L) leads to faster reaction as more radicals are quickly formed [32]. However, there are two significant disadvantages in using very high concentration of H<sub>2</sub>O<sub>2</sub> (above 10 ml/L). Firstly, due to its overabundance relative to the dye pollutant, most of H<sub>2</sub>O<sub>2</sub> would not have any substrate to act upon and would, therefore, be wasted. Secondly, high concentration of H<sub>2</sub>O<sub>2</sub> decreases dye decolorization because unreacted H<sub>2</sub>O<sub>2</sub> acts as a scavenger of  $\bullet\text{OH}$  and produces less potent peroxy radicals, as shown in Eq. (4) [33]:



A similar observation was reported concerning the wet hydrogen peroxide catalytic oxidation of MB with CuS nanocrystals/reduced graphene oxide [33(b)].

#### 3.3.4. Effect of initial concentration of MB

The effect of initial concentration of MB on its decolorization is displayed in Figure 5(e). When increasing the dye concentration from 20 ppm to 200 ppm, a decrease of its reactivity is observed. At 20 ppm MB concentration, 100% decolorization is observed within 60 min; at 50 ppm, in 90 min; at 100 ppm, in 120 min. For MB concentrations of 150 and 200 ppm, the decolorization percentages are about 87 and 81 in 120 min, respectively. This is explainable by the fact that when the production of hydroxyl radicals is constant, yet dye concentration increases, the relative number of free radicals attacking the dye molecules decreases [34].

#### 3.3.5. Effect of pH of dye solution

Figure 5(f) illustrates the influence of the solution pH on the decolorization of MB dye using CuO/FAZ-X. The decolorization percentage increases from pH 4 to 7, and then decreases. MB shows the maximum decolorization % at pH 6.8 (natural) in 120 min.

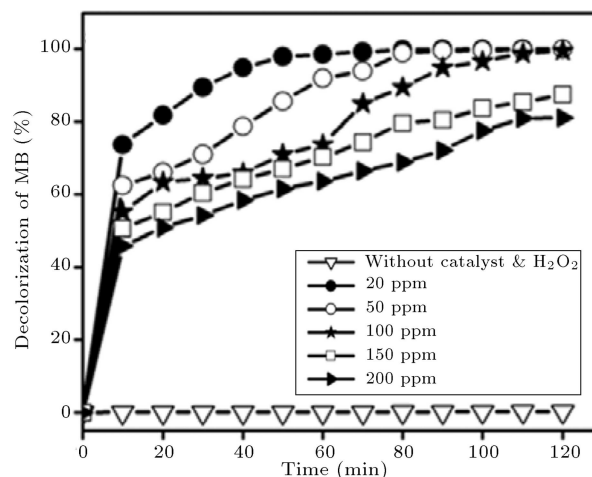


**Figure 5e.** Effect of initial dye concentration on MB decolorization by CuO/FAZ-X (conditions: 5 ml/L H<sub>2</sub>O<sub>2</sub>, catalyst dosage 250 mg/L, and pH 6.8).

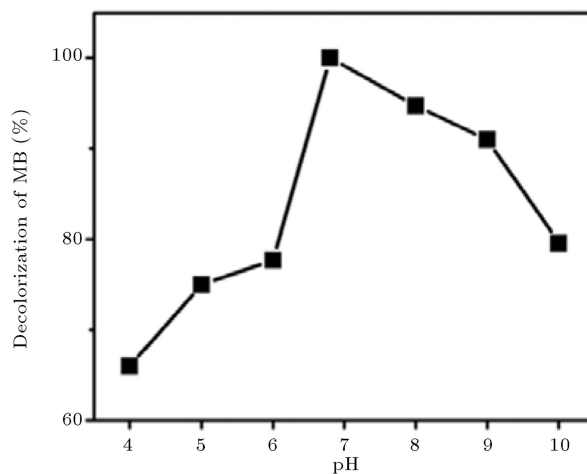


**Figure 5f.** Effect of pH on MB decolorization by CuO/FAZ-X (conditions: 5 ml/L H<sub>2</sub>O<sub>2</sub>, catalyst dosage 250 mg/L, and 100 ppm dye).

This trend can be explained on the basis of zero-point charge ( $\text{pH}_{\text{zpc}}$ ) and the acid/base property of the catalyst surface. Since  $\text{pH}_{\text{zpc}}$  for CuO/FAZ-X is 7.3, the surface of the catalyst is presumably positively and negatively charged in acidic and alkaline solutions, respectively [33].

MB is a cationic/basic dye. MB molecule is stable in acidic condition, but unstable in alkaline pH (above 10). At acidic pH ( $< 6.8$ ), there exists electrostatic repulsion between cationic MB molecule and the positive charge of the catalyst surface [34]. Hence, MB molecule cannot approach the surface of the catalyst, where hydroxyl radicals are produced. Consequently, the decolorization efficiency is less/decreased. Moreover, at acidic pH, the anion  $\text{Cl}^-$  is able to react with  $\text{HO}\bullet$  radical leading to  $\text{ClO}\bullet\text{-H}$  radical ion. This  $\text{ClO}\bullet\text{-H}$  radical anion has a much lower reactivity than  $\text{HO}\bullet$ . Due to this phenomenon, the decolorization percentage

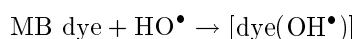


of MB could decrease [34,35]. At pH above  $pH_{zpc}$  (alkaline condition), the surface of the catalyst becomes negatively charged by losing protons. Therefore, the adsorption of MB reaches its maximum value due to strong electrostatic attraction [36], and hence MB is stabilized. Furthermore, the production of hydroxyl radicals (due to the reaction of hydroxyl radicals with hydroxide ions) decreases at the alkaline medium, which in turn decreases the decolorization efficiency. In addition, the strong MB adsorption leads to a major decrease in the active centers, and consequently to a decrease in the production of hydroxyl radical on the catalyst surface [37]. When  $pH > 10$ , the decolorization of MB is inhibited. This is because the hydroxide ions compete with MB molecule in adsorption on the surface of catalyst. In addition, there are two inhibiting aspects. First,  $OH^-$  reacts with  $HO^\bullet$  to form  $HO_2^\bullet$ , which has very low reactivity with dye. Second,  $H_2O_2$  decomposes into  $H_2O$  and  $O_2$  at higher pH [37]. Thus, based on the above results and discussions, neutral pH 6.8 (original pH of the MB solution) is selected as the optimal value which facilitates 100% decolorization.

### 3.4. Reaction mechanism

Decolorization experiment clearly suggests that CuO and FAZ-X undergo synergic effect on catalytic activity, making the combined catalyst CuO/FAZ-X capable of reacting effectively with hydrogen peroxide and producing more  $OH^\bullet$ . The heterogeneous activation of hydrogen peroxide can be expressed in Eqs. (5) to (7), and Figure 6. Oxidation-reduction reactions in the redox couple Cu(II)/Cu(I) take place in the presence of excessive hydrogen peroxide forming reactive hydroxyl ( $OH^\bullet$ ) and hydroperoxyl ( $HO_2^\bullet$ ) radicals. These

hydroxyl radicals attack the MB dye and degrade it to give several intermediate products. Finally, MB dye is completely decolorized [30].



### 3.5. Catalyst recycling experiments

Catalyst recycling experiments were performed to study the stability and sustainability of the catalyst during the decolorization process (Figure 7).

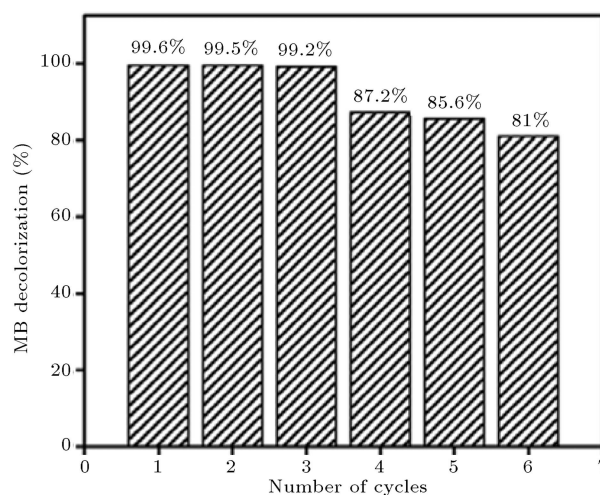


Figure 7. Reusability study of CuO/FAZ-X.

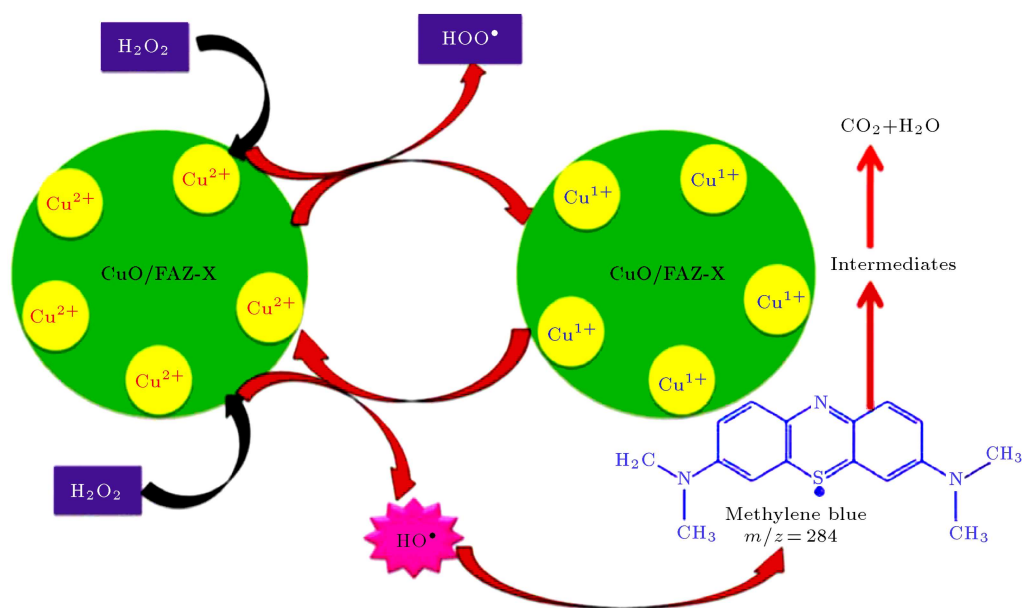


Figure 6. Possible catalytic process of CuO/FAZ-X for the oxidative decolorization of MB.

**Table 4.** Compilation of performances of various heterogeneous catalysts for MB decolorization by CWPO process.

| Catalysts   | Operating conditions   | Time (h) | Decolorization (%) | Recycle run | Ref.          |
|---|--|----------|--------------------|-------------|---------------|
| Layered manganese oxide (Na-OL-1)                               | [Catalyst] = 200 mg/L<br>[H <sub>2</sub> O <sub>2</sub> ] <sub>o</sub> = 55 ml/L<br>[MB] <sub>o</sub> = 30 ppm<br>T = 25°C, pH = 7.6                       | 1        | 98                 | —           | [36]          |
| $\alpha$ -Fe <sub>2</sub> O <sub>3</sub> /MCM-41 nano composite | [Catalyst] = 1000 mg/L<br>[H <sub>2</sub> O <sub>2</sub> ] <sub>o</sub> = 4 ml/L<br>[MB] <sub>o</sub> = 10 ppm<br>T = 25°C, pH = 4                         | 1.5      | 97                 | —           | [37]          |
| Fe <sub>3</sub> O <sub>4</sub> /reduced graphene oxide          | [Catalyst] = 300 mg/L<br>[H <sub>2</sub> O <sub>2</sub> ] <sub>o</sub> = 60 mM<br>[MB] <sub>o</sub> = 10 ppm<br>T = 25°C, pH = Natural                     | 2        | 98.6               | 5           | [38]          |
| TiO <sub>2</sub> /manganese oxide composites                    | [Catalyst] = 500 mg/L<br>[H <sub>2</sub> O <sub>2</sub> ] <sub>o</sub> = 30 ml/L<br>[MB] <sub>o</sub> = 10 ppm<br>T = 25°C, pH = Natural                   | 2        | 96.4               | —           | [39]          |
| 4A zeolite-zero valent iron nano particle (nZVI/4A zeolite)     | [Catalyst] = 200 mg/L<br>[H <sub>2</sub> O <sub>2</sub> ] <sub>o</sub> = 10 mM<br>[MB] <sub>o</sub> = 30 ppm<br>T = 25°C, pH = 3                           | 3        | 100                | 3           | [40]          |
| MnOx/WO <sub>3</sub> nanoparticles                              | [Catalyst] = 200 mg/L<br>[H <sub>2</sub> O <sub>2</sub> ] <sub>o</sub> = 200 ml/L<br>[MB] <sub>o</sub> = 10 ppm<br>T = 25°C, pH = Natural                  | 1        | 100                | 4           | [41]          |
| CuS/rGO composite   | [Catalyst] = 200 mg/L<br>[H <sub>2</sub> O <sub>2</sub> ] <sub>o</sub> = 0.08 M<br>[MB] <sub>o</sub> = 10 ppm<br>T = 25°C, pH = 7                          | 1.5      | 93                 | 5           | [42]          |
| Fe <sub>2</sub> O <sub>3</sub> /attapulgite                     | [Catalyst] = 10 g/L<br>[H <sub>2</sub> O <sub>2</sub> ] <sub>o</sub> = 0.098 M<br>[MB] <sub>o</sub> = 100 ppm<br>T = 20°C, pH = 5                          | 1.5      | 100                | 10          | [43]          |
| CuO/fly ash converted zeolite X                                 | [Catalyst] = 250 mg/L<br>[H <sub>2</sub> O <sub>2</sub> ] <sub>o</sub> = 5 ml/L<br>[MB] <sub>o</sub> = 100 ppm<br>T = room temperature, pH = natural (6.8) | 2        | 100                | 6           | Present study |

Decolorization experiments were repeated for 6 cycle using the same CuO/FAZ-X catalyst sample which was washed every time with water and dried at 100°C before reuse. As observed from Figure 7, there was no apparent loss of the catalytic activity during the first 3 cycles. But, during the fourth run, much longer time was required to obtain complete decolorization (100%) of MB. The slight decrease in catalytic activity from fourth cycle onward might have been caused by the loss of catalyst during handling and regeneration and/or incomplete removal of by-products during washing. Nevertheless, the results indicate that there is almost no appreciable activity loss of the catalyst during 6

recycles. The physico-chemical stability was checked by FTIR spectrum of the used catalyst (Figure 8). This has similarity to the spectrum of fresh CuO/FAZ-X. Also, in the FTIR spectrum of the used catalyst, no characteristic peaks from MB could be found. FTIR study, thus, shows that the catalyst material is chemically stable on reuse. A comparison was made between the results of efficiency and reusability of the present catalyst with those of the reported catalysts in literature [36-43], and the relevant data are compiled in Table 4. The present CuO/FAZ-X catalyst has certainly good stability and sustainability over the previous catalysts.

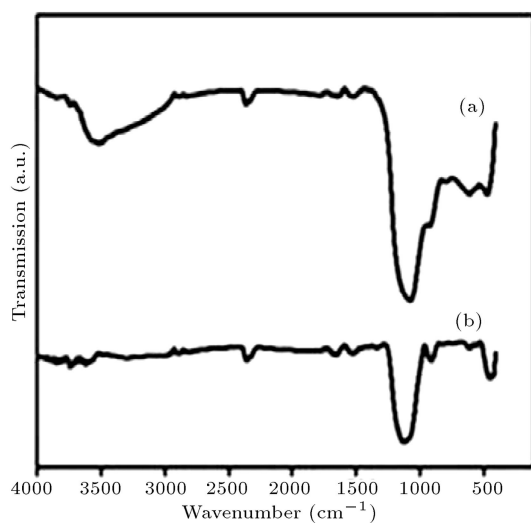


**Figure 8.** FTIR spectra of CuO/FAZ-X catalyst before and after decolorization of MB.

### 3.6. LC-MS with ESI-Mass studies for product analysis

The intermediates generated during MB decolorization were analyzed using HPLC-(ESI)-TOF-MS which allowed the detection of aromatic compounds with different molecular weights. Figures 9(a) and 9(b) show ESI-mass spectra of samples from wet catalytic oxidation of MB before and after the reaction in 120 min. The fresh MB (Figure 9(a)) gives a single peak at  $m/z = 284$  corresponding to  $M^+$  molecular ion of MB. The peaks at  $m/z = 285$ , 286 are a result of  $C^{13}$  and  $S^{34}$  isotopes in the MB molecule. After 120 min reaction time in the presence of  $H_2O_2$  under dark condition, the MB dye parent peak is declined/vanished, and various new peaks (Figure 9(b)) arise, indicating that the MB dye is broken down and new products are formed. The peaks at  $m/z = 384$ , 487 correspond to dimer of azure A, and azure C from MB molecule [44]. The LC-MS

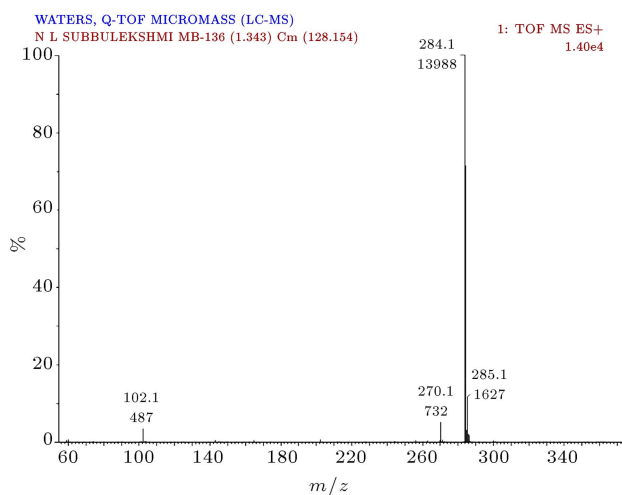


**Figure 9a.** HPLC-ESI-MS spectrum of fresh MB dye.

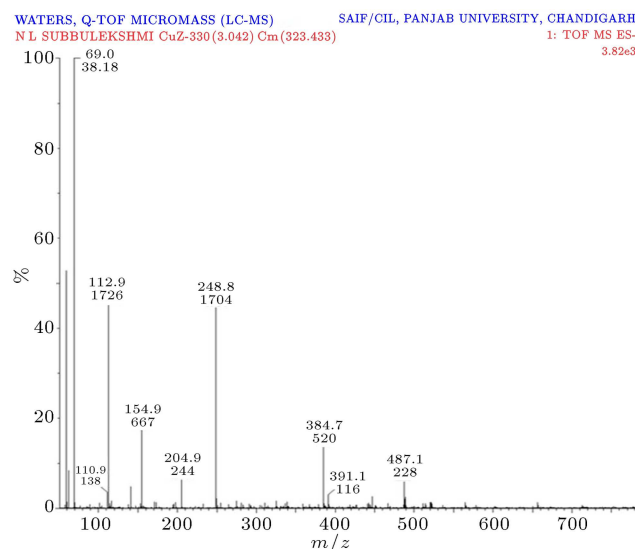


**Figure 9b.** HPLC-ESI-MS spectra of products from MB decolorization for 120 min 100 ppm MB, and pH 6.8.

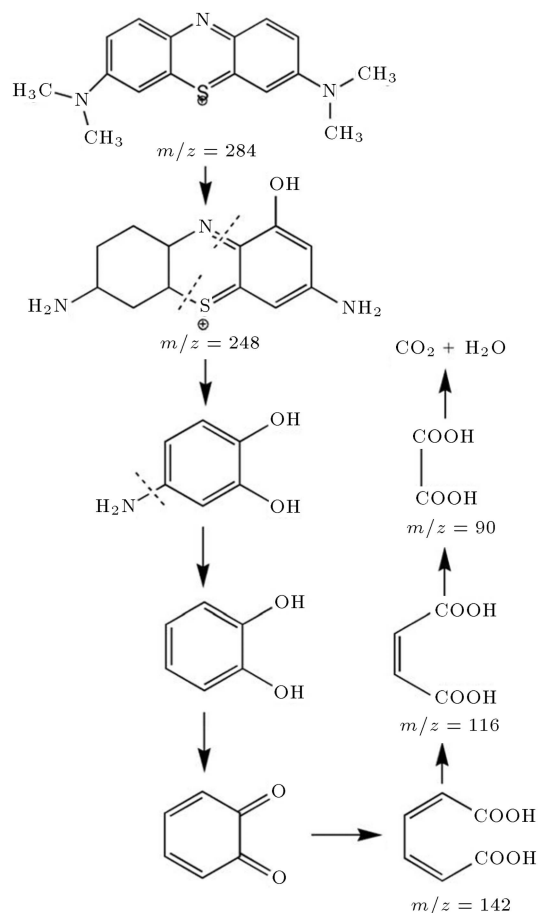


**Figure 10.** Oxidative decolorization pathway of MB dye.

analysis results suggest a sequence of oxidation reaction mechanism (Figure 10), in which the hydroxyl radical preferentially attacks the chromophoric centers of the dye molecule. Finally, ring opening of aromatic rings takes place and the intermediates lead to the formation

of organic acids (formic acid) converted into  $\text{CO}_2$  and  $\text{H}_2\text{O}$  [45].

### 3.7. COD studies

Apart from LC-MS analysis, COD is also used for confirming the decolorization of MB dye. The COD test allows the measurement of dye in terms of the total quantity of oxygen required for the oxidation of dye organic matters. The COD removal of the reaction mixture after MB decolorization over CuO/FAZ-X (optimal conditions  $\text{H}_2\text{O}_2 = 5 \text{ ml/L}$ ,  $250 \text{ mg/L}$  catalyst,  $100 \text{ ppm}$  MB,  $\text{pH} = 6.8$ , ambient temperature) was 73.6% for 2 h, 80.3% for 4 h, and 95% for 8 h (Figure 11). The COD reduction is less than the percentage of decolorization, which may be due to the formation of smaller uncolored products. Therefore, it is apparent that for complete mineralization of MB dye, longer reaction time is required. This result is not new, but has already been reported in many previous studies [21,27,33(b)]. The COD and LC-MS results are in agreement, confirming the decolorization of the MB molecule into small fragments.

### 3.8. Comparison of CWPO activities of different catalysts

In order to realize and appreciate the CWPO performance/activity of the present catalyst CuO/FAZ-X, a comparison of efficiencies of the present and literature-reported [36-43] catalysts in MB dye decolorization is made. Table 4 compiles the decolorization % of MB along with the experimental conditions employed. Considering the higher concentration (100 ppm) of the MB employed in the present study (compared to 10 ppm in many other studies), the data in Table 4 certainly reveal that CuO/FAZ-X catalyst in the present study has an outstanding performance.

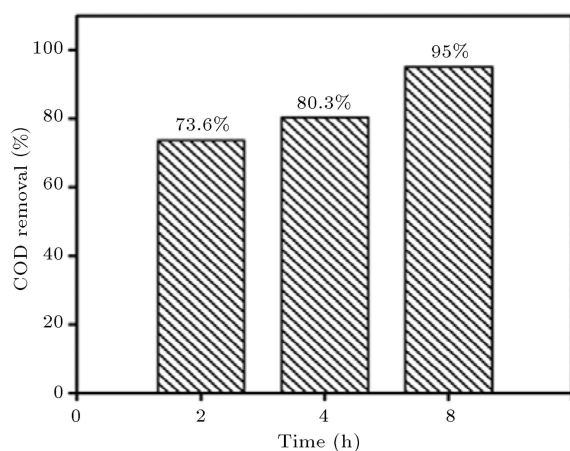


**Figure 11.** % Removal COD Versus time (ambient condition:  $5 \text{ ml/L}$   $\text{H}_2\text{O}_2$ ,  $250 \text{ mg/L}$  CuO/FAZ-X,  $100 \text{ ppm}$  dye, and  $\text{pH} 6.8$ ).

## 4. Conclusions

In this work, the cheap and easily available waste material coal Fly Ash was converted into Zeolite X type (FAZ-X) and CuO was incorporated to design a new catalyst (CuO/FAZ-X). All the instrumental characterizations proved the formation of CuO incorporated FAZ-X. Employing CuO, FAZ-X, and CuO/FAZ-X as heterogeneous Fenton catalysts for wet catalytic oxidative decolorization of MB in the presence of  $\text{H}_2\text{O}_2$ , it was found that CuO/FAZ-X exhibits more than twice the efficiency of either FAZ-X or CuO. In fact, CuO incorporation leads to synergic effect with zeolite and dramatically improves the catalytic efficiency of CuO/FAZ-X. Hence, the novel catalyst has many advantages such as simple preparation, remarkable performance, good structural stability, and sustainable catalytic activity in repetitive reaction cycles. So, CuO/FAZ-X is an eco-friendly green catalyst developed from the waste material coal fly ash. Thus, the present work demonstrates a simple and facile route for the conversion of waste coal fly ash into a valuable catalyst.

## References

- Suraja, P.V., Yaakob, Z., Binitha, N.N., Triwahyono, S. and Siliya, P.P. "Co<sub>3</sub>O<sub>4</sub> doped over SBA 15: excellent adsorbent materials for the removal of methylene blue dye Pollutant", *Clean. Techn. Environ. Policy.*, **15**, pp. 967-975 (2013).
- Guyer, G.T. and Ince, N.H. "Degradation and toxicity reduction of textile dyestuff by ultrasound", *Ultrason. Sonochem.*, **10**, pp. 235-240 (2003).
- Verma, A.K., Dash, R.R. and Bhunia, P. "A review on chemical coagulation/flocculation technologies for removal of colour from textile wastewaters", *J. Environ. Manage.*, **93**, pp. 154-168 (2012).
- Sun, J.H., Sun, S.P., Wang, G.L. and Qiao, L.P. "Degradation of azo dye Amido black 10B in aqueous solution by Fenton oxidation process", *Dyes. Pigments.*, **74**, pp. 647-652 (2007).
- Liu, S.Q., Feng, L.R., Xu, N., Chen, Z.G. and Wang, X.M. "Magnetic nickel ferrite as a heterogeneous photo-Fenton catalyst for the degradation of rhodamine B in the presence of oxalic acid", *Chem. Engg. J.*, **203**, pp. 432-439 (2012).
- Demir, N., Gündüz, G. and Dükkanc, M. "Degradation of a textile dye, Rhodamine 6G (Rh6G), by heterogeneous sonophoto Fenton process in the presence of Fe-containing TiO<sub>2</sub> catalysts", *Environ. Sci. Pollut. Res.*, **22**, pp. 3193-3201 (2015).
- Ince, N.H.G. and Tezcanli, G. "Reactive dyestuff degradation by combined sonolysis and ozonation", *Dyes. Pigments.*, **49**(3), pp. 145-153 (2001).
- Ribeiro, R.S., Silva, A.M.T., Figueiredo, J.L., Faria, J.L. and Gomes, H.T. "Catalytic wet peroxide oxidation: a route towards the application of hybrid

- magnetic carbon nanocomposites for the degradation of organic pollutants - A review", *Appl. Catal. B: Environ.*, **187**, pp. 428-460 (2016).
9. Ye, W., Zhao, B., Gao, H., Huang, J. and Zhang, X. "Preparation of highly efficient and stable Fe, Zn, Al-pillared montmorillonite as heterogeneous catalyst for catalytic wet peroxide oxidation of orange II", *J. Porous. Mater.*, **23**, pp. 301-310 (2016).
  10. Munoz, M., de Pedro, Z.M., Casas, J.A. and Rodriguez, J.J. "Preparation of magnetite-based catalysts and their application in heterogeneous Fenton oxidation - A review", *Appl. Catal. B: Environ.*, **176-177**, pp. 249-265 (2016).
  11. (a) Rodrigues, C.S.D., Carabineiro, S.A.C., Maldonado-Hodar, F.J. and Madeira, L.M. "Wet peroxide oxidation of dye-containing wastewaters using nanosized Au supported on  $\text{Al}_2\text{O}_3$ ", *Catal. Today*. (2016), <http://dx.doi.org/10.1016/j.cattod.2016.06.031>;  
(b) Kong, L., Zhou, X., Yao, Y., Jian, P. and Diao, G. "Catalytic wet peroxide oxidation of aniline in wastewater using copper modified SBA-15 as catalyst", *Environ. Technol.*, **37**(3), pp. 422-429 (2016).
  12. Drasinac, N., Erjavac, B., Drazic, G. and Pintar, A. "Peroxo and gold modified titanium nanotubes for effective removal of methyl orange with CWPO under ambient conditions", *Catal. Today* (2016), <http://dx.doi.org/10.1016/j.cattod.2016.06.038>.
  13. (a) Ji, F., Li, C. and Den, L. "Performance of CuO/Oxone system: Heterogeneous catalytic oxidation of phenol at ambient conditions", *Chem. Engg. J.*, **178**, pp. 239-243 (2011);  
(b) Singh, L., Rekha, P. and Chand, S. "Cu-impregnated zeolite y as highly active and stable heterogeneous Fenton-like catalyst for degradation of congo red dye", *Sep. Purif. Technol.*, **170**, pp. 321-336 (2016).
  14. Tehrani-Bagha, A.R., Gharagozlou, M. and Emami, F. "Catalytic wet peroxide oxidation of a reactive dye by magnetic copper ferrite nanoparticles", *J. Environ. Chem. Eng.*, **4**, pp. 1530-1536 (2016).
  15. Bradu, C., Frunza, L., Mihalche, N., Avramescu, S.M., Neat, M. and Udrea, I. "Removal of reactive black 5 azo dye from aqueous solutions by catalytic oxidation using CuO/ $\text{Al}_2\text{O}_3$  and NiO/ $\text{Al}_2\text{O}_3$ ", *Appl. Catal. B: Environ.*, **96**, pp. 548-556 (2010).
  16. Alvarez, P.M., McLurgh, D. and Plucinski, P. "Copper oxide mounted on activated carbon for wet air oxidation of aqueous phenol 1. Kinetic and mechanistic approaches", *Ind. Eng. Chem. Res.*, **41**, pp. 2147-2152 (2002).
  17. Bo, L., Liao, J., Zhang, Y., Wang, X. and Yang, Q. "CuO/zeolite catalyzed oxidation of gaseous toluene under microwave heating", *Front. Environ. Sci. Eng.*, **7**(3), pp. 395-402 (2013).
  18. Vijaikumar, S., Subramanian, T. and Pitchumani, K. "Zeolite Encapsulated Nanocrystalline CuO: A redox catalyst for the oxidation of secondary alcohols", *J. Nanomater.*, DOI: 10.1155/2008/257691 (2008).
  19. Brazlauskas, M. and Kitrys, S. "Synthesis and properties of CuO/Zeolite sandwich type adsorbent-catalysts", *Chin. J. Catal.*, **29**(1), pp. 25-30 (2008).
  20. Lin, K.S. and Wang, H.P. "Byproduct shape selectivity in supercritical water oxidation of 2-Chlorophenol effected by CuO/ZSM-5", *Langmuir*, **16**, pp. 2627-2633 (2000).
  21. Nezamzadeh-Ejhieh, A. and Salimi, Z. "Heterogeneous photodegradation catalysis of o-phenylenediamine using CuO/Xzeolite", *Appl. Catal. A: Gen.*, **390**, pp. 110-118 (2010).
  22. Wang, S.B. and Wu, H.W. "Environmental-benign utilisation of fly ash as low-cost adsorbents", *J. Hazard. Mater.*, **136**, pp. 482-501 (2006).
  23. Amaladhas, T.P. and Thavamani, S.S. "Encapsulation of N, N'-ethlenebis(salicylamide) metal complexes in fly ash based zeolite, characterization and catalytic activity", *Adv. Mat Lett.*, **4**(9), pp. 688-695 (2013).
  24. Ojha, K., Pradhan, N.C. and Samantha, A. "Zeolite from fly ash: synthesis and characterization", *Bull. Mater. Sci.*, pp. 555-564 (2004).
  25. (a) APHA, AWWA (American Public Health Association), Standard Methods for the Examination of Water and Wastewater, American Public Health Association, Washington D.C (1998);  
(b) ASTM, *ASTM Standard Specification for Coal fly Ash and Raw or Calcined Natural Pozzolan for Use in Concrete (C618-05)*, In Annual Book of ASTM Standards, Concrete and Aggregates, **04.02.**, American Society for Testing Materials, USA (2005).
  26. Ting, C., Zhifeng, L., Xuerong, Z., Zhichao, L., Yajun, L., Wei, L. and Bo, W. "Zeolite-based CuO nanotubes catalyst: investigating the characterization, mechanism, and decolorisation process of methylene blue", *J. Nanopart. Res.*, **16**, pp. 2608 (2014).
  27. Nezamzadeh-Ejhieh, A. and Shamsabadi, M.K. "Comparison of photocatalytic efficiency of supported CuO onto micro and nano particles of zeolite X in photodecolorization methylene blue and methyl orange aqueous mixture", *Appl. Catal. A: Gen.*, **477**, pp. 83-92 (2014).
  28. Liou, R.M. and Chen, S.H. "CuO impregnated activated carbon for catalytic wet peroxide oxidation of phenol", *J. Hazard. Mater.*, **172**, pp. 498-506 (2009).
  29. Jalil, A.A., Satar, M.A.H., Triwahyono, S., et al. "Tailoring the current density to enhance photocatalytic activity of CuO/HY for decolorization of malachite green", *J. Electroanal. Chem.*, **701**, pp. 50-58 (2013).
  30. Fathima, N.N., Aravindhan, R., Rao, J.R. and Nair, B.U. "Dye house wastewater treatment through advanced oxidation process using Cu-exchanged Y zeolite: A heterogeneous catalytic approach", *Chemosphere.*, **70**, pp. 1146-1151 (2008).

31. Nezamzadeh-Ejehieh, A. and Shamsabadi, M.K. "Decolorization of binary azo dyes mixture using CuO incorporated nanozeolite-X as a heterogeneous catalyst under solar irradiation", *Chem. Eng. J.*, **228**, pp. 631-641 (2013).
32. Valkaj, K.M., Katovic, A. and Zrncevi, S. "Catalytic properties of Cu/13X zeolite based catalyst in catalytic wet peroxide oxidation of phenol", *Ind. Eng. Chem. Res.*, **50**, pp. 4390-4397 (2011).
33. (a) Subbaramaiah, V., Srivastava, V.C. and Mall, I.D. "Optimization of reaction parameters and kinetic modeling of catalytic wet peroxidation of Picoline by Cu/SBA-15", *Ind. Eng. Chem. Eng.*, **52**, pp. 9021-9029 (2013);  
(b) Qian, J., Wang, K., Guan, Q., Li, H., Xu, H. and Liu, Q. "Enhanced wet hydrogen peroxide catalytic oxidation performances based on CuS nanocrystals/reduced graphene oxide composites", *Appl. Surf. Sci.*, **288**, pp. 633-640 (2014).
34. Zhou, S., Gu, C., Qian, Z., Xu, J. and Xia, C. "The activity and selectivity of catalytic peroxide oxidation of chlorophenols over Cu-Al hydrotalcite/clay composite", *J. Colloid. Interface. Sci.*, **357**, pp. 447-452 (2011).
35. Nezamzadeh-Ejehieh, A. and Hushmandrad, Sh. "Solar photodecolorization of methylene blue by CuO/X zeolite as a heterogeneous catalyst", *Appl. Catal A: Gen.*, **388**, pp. 149-159 (2010).
36. Zhang, L., Nie, Y., Chun Hu, C. and Hu, X. "Decolorization of methylene blue in layered manganese oxide suspension with H<sub>2</sub>O<sub>2</sub>", *J. Hazard. Mater.*, **190**, pp. 780-785 (2011).
37. Ursachi, I., Stancu, A. and Vasile, A. "Magnetic  $\alpha$ -Fe<sub>2</sub>O<sub>3</sub>/MCM-41 nanocomposites: Preparation, characterization, and catalytic activity for methylene blue degradation", *J. Colloid. Interface. Sci.*, **377**, pp. 184-190 (2012).
38. Liu, W., Qian, J., Wang, K., Xu, H., Jiang, D., Liu, Q., Yang, X. and Li, H. "Magnetically separable Fe<sub>3</sub>O<sub>4</sub> nanoparticles-decorated reduced graphene oxide nanocomposite for catalytic wet hydrogen peroxide oxidation", *J. Inorg. Organomet. Polym.*, **23**, pp. 907-916 (2013).
39. Park, J.H., Jang, I., Song, K. and Oh, S.G. "Surfactants-assisted preparation of TiO<sub>2</sub>-Mn oxide composites and their catalytic activities for degradation of organic pollutant", *J. Phy. Chem. Solid.*, **74**, pp. 1056-1062 (2013).
40. Wu, Y., Yang, M., Hu, S., Wang, L. and Yao, H. "Characteristics and mechanisms of 4A zeolite supported nanoparticulate zero-valent iron as Fenton-like catalyst to degrade methylene blue", *Toxicol. Environ. Chem.*, **96**(2), pp. 227-242 (2014).
41. Amini, M., Pourbadiei, B., Ruberu, T.P.A. and Keith Woo, L. "Catalytic activity of MnOx/WO<sub>3</sub> nanoparticles: synthesis, structure characterization and oxidative degradation of methylene blue", *New J. Chem.*, **38**, pp. 1250-1255 (2014).
42. Qian, J., Wang, K., Guan, Q., Li, H., Xu, H., Liu, Q., Liu, W. and Qiu, B. "Enhanced wet hydrogen peroxide catalytic oxidation performances based on CuS nanocrystals/reduced graphene oxide composites", *Appl. Surf. Sci.*, **288**, pp. 633-640 (2014).
43. Zhangab, T. and Nana, Z.R. "Decolorization of methylene blue and congo red by attapulgite-based heterogeneous Fenton catalyst", *Desalin. Water. Treat.*, pp. 1-8 (2014). DOI: 10.1080/19443994.2014.992969.
44. Meetani, A.M., Khaleel, A. and Ahmed, A. "Photocatalytic degradation of methylene blue using a mixed catalyst and product analysis by LC/MS", *Chem. Eng. J.*, **157**, pp. 373-378 (2010).
45. Wang, Q., Tian, S. and Ning, P. "Degradation mechanism of methylene blue in a heterogeneous Fenton-like reaction catalyzed by Ferrocene", *Ind. Eng. Chem. Res.*, **5**, pp. 643-649 (2014).

## Biographies

**Esakkiappan Subramanian** is currently Professor and the Head of the Department of Chemistry, Manonmanian Sundaranar University, Tirunelveli, India. He obtained his PhD degree from University of Madras in 1989. He has about 26 years of teaching and research experience. His research interests include chemical sensors, photocatalysis, and environmental water pollution studies.

**Nallsivam Lekshmi Subbulekshmi** received her MSc degree in Chemistry from Annamalai University, Annamalai Nagar, Tamil Nadu, in 2004, and MPhil degree from Manonmaniam Sundaranar University, Tirunelveli, Tamil Nadu, in 2006. She is currently working on her PhD in Chemistry under the supervision of Professor Dr. E. Subramanian in Chemistry Department at Manonmaniam Sundaranar University, Tirunelveli, India. Her research interests include synthesis of heterogeneous catalysts from waste materials, zeolites, zeolite based photocatalysts, photocatalysis, catalysis and environmental applications.